Dyes and Pigments 91 (2011) 79–88

Contents lists available at ScienceDirect

Dyes and Pigments

journal homepage: www.elsevier.com/locate/dyepig

Novel aminated benzimidazo[1,2-*a*]quinolines as potential fluorescent probes for DNA detection: Microwave-assisted synthesis, spectroscopic characterization and crystal structure determination

Nataša Perin [a], Marijana Hranjec [a,*], Gordana Pavlović [b], Grace Karminski-Zamola [a,**]

[a] Department of Organic Chemistry, University of Zagreb, Marulićev trg 20, P.O. Box 177, HR-10000 Zagreb, Croatia
[b] Department of Applied Chemistry, University of Zagreb, Prilaz baruna Filipovića 28a, HR-10000 Zagreb, Croatia

ARTICLE INFO

Article history:
Received 5 November 2010
Received in revised form
2 February 2011
Accepted 3 February 2011
Available online 2 April 2011

Keywords:
Benzimidazoles
Benzimidazo[1,2-*a*]quinolines
Microwave synthesis
Amination
Crystal structure determination
Interaction with ct-DNA

ABSTRACT

A synthesis of novel benzimidazo[1,2-*a*]quinolines, substituted with piperidine, pyrrolidine and piperazine nuclei has been accomplished using an uncatalyzed amination protocol under microwave heating. All compounds were characterized by means of ^{1}H, ^{13}C NMR, IR, UV/Vis and fluorescence spectroscopy. Crystal and molecular structures of 2-chloro- and 2-piperidinyl-benzimidazo[1,2-*a*]quinoline-6-carbonitrile were determined by X-ray diffractometry. These molecules are essentially planar. Their molecular assembly is characterized by the existence of weak intermolecular hydrogen bonds of C–H···N type and π–π aromatic interactions. The π–π aromatic stacking observed in the solid state structures of the 2-chloro- and 2-piperidinyl- derivatives are not analogous. The spectroscopic properties of these amino substituted benzimidazo[1,2-*a*]quinolines as their hydrochloride salts in the presence of ct-DNA were studied by means of fluorescence spectroscopy. Comparison of binding properties of amino substituted benzimidazo [1,2-*a*]quinoline hydrochloride salts to ct-DNA revealed significantly enhanced fluorescence emission intensity and thus offer the potential applications as a DNA-specific fluorescent probes.

1. Introduction

In recent years substituted benzimidazoles and their azino fused derivatives have been one of the most extensively studied classes of heterocyclic compounds. The permanent and growing interest in their synthesis is a direct consequence of their well known biological activities [1–5]. Besides the fact that benzimidazoles are widely incorporated in the structure of numerous important medical and biochemical agents, they exhibit structural similarity with some naturally occurring compounds such as purine and, therefore, can easily interact with biomolecules [6,7]. Due to their planar structure, they have ability to intercalate between adjacent base pairs of a DNA molecule and thus offer a potential application as fluorescent probes in homogeneous assays of biological molecules [8–10]. Nowadays, optical biomarkers are widely used in biochemical and medicinal studies for the detection of biologically important molecules such as DNA, RNA, proteins and enzymes. Detection of biomolecules based upon fluorescence has received much attention, due to the notable progress in fluorescence instrumentation as well as in the synthesis of different fluorophores. Since benzannulated benzimidazoles usually posses a highly conjugated planar chromophore, other important application areas of this class of compounds are in optoelectronics, optical lasers, organic luminophores or fluorescent dyes in traditional textile and polymer fields [11–16]. Microwave assisted chemistry has greatly expanded over the last few years and has been used for the rapid synthesis of a variety of organic compounds [17–20]. Microwave assisted organic reactions have been proven to be much quicker than those relying upon conventional heating [21,22]. Moreover, microwave assisted amination of arylhalides has become an important and frequently required reaction in the synthesis of *N*-aryl substituted organic molecules in many research fields such as medicinal and pharmaceutical chemistry, dyes, optoelectronics and electronic materials [23–26].

All of the above mentioned considerations prompted us to synthesize novel aminated benzimidazo[1,2-*a*]quinolines using an uncatalyzed microwave assisted amination. The investigation is the part of our continuing research on the synthesis of benzimidazole derivatives. The amination reaction was carried out upon the common precursor **4** which was prepared photochemically from its non-fused benzimidazole derivative **3** which in turn was derived

* Corresponding author. Tel.: +385 14597245; fax: +385 14597250.
** Corresponding author. Tel.: +385 14597215; fax: +385 14597224.
E-mail addresses: mhranjec@fkit.hr (M. Hranjec), gzamola@fkit.hr (G. Karminski-Zamola).

0143-7208/$ – see front matter © 2011 Elsevier Ltd. All rights reserved.
doi:10.1016/j.dyepig.2011.02.003

from the condensation between cyanomethylbenzimidazole **1** and aldehyde **2**. Although the one-pot synthesis of chloro-substituted benzimidazo[1,2-*a*]quinoline **4** has recently been reported by a copper-catalyzed cascade reactions [27], we have rather used a photochemical environmentally friendly approach, using ethanol as a less toxic solvent in comparison with solvents used in the above mentioned synthesis (DMF, DMSO) and without any additionally necessary catalysts or ligands.

2. Experimental

2.1. General methods

All chemicals and solvents were purchased from commercial suppliers. Melting points were recorded on an Original Keller Mikroheitztisch apparatus (Reichert, Wien) and Büchi 535. ^{1}H and ^{13}C NMR spectra were recorded on a Varian Gemini 300 or Varian Gemini 600 at 300, 600 and 150 and 75 MHz, respectively. All NMR spectra were measured in DMSO-d_6 solutions using TMS as an internal standard. Chemical shifts are reported in ppm (δ) relative to TMS. In preparative photochemical experiments the irradiation was performed at room temperature with a water-cooled immersion well with an "Origin Hanau" 400-W high-pressure mercury arc lamp using Pyrex glass as a cut-off filter of wavelengths below 280 nm. Microwave-assisted synthesis was performed in a Milestone start S microwave oven using quartz cuvettes under the pressure of 40 bar. All compounds were routinely checked by TLC with Merck silica gel 60F-254 glass plates. Elemental analysis for carbon, hydrogen and nitrogen were performed on a Perkin–Elmer 2400 elemental analyzer.

2.2. Synthesis

2.2.1. 2-Chloro-benzimidazo[1,2-a]quinoline-6-carbonitrile 4[27]

An ethanolic solution (400 mL) of compound **3** (0.900 g, 2.87 mmol) was irradiated at room temperature, with 400 W high-pressure mercury lamp, using a Pyrex filter for 10 h [28,29]. The obtained product was filtered off to give 0.432 g (54%) of yellow crystals; m.p. 288–291 °C. IR (diamond): ν/cm^{-1} = 2361, 2235, 1598, 1535; ^{1}H NMR (DMSO-d_6, 600 MHz): δ/ppm = 8.80 (s, 1H, $H_{arom.}$), 8.73 (d, 1H, J = 7.5 Hz, $H_{arom.}$), 8.70 (s, 1H, $H_{arom.}$), 8.16 (d, 1H, J = 8.5 Hz, $H_{arom.}$), 8.02 (d, 1H, J = 8.3 Hz, $H_{arom.}$), 7.73 (d, 1H, J = 8.43 Hz, $H_{arom.}$), 7.66–7.57 (m, 2H, $H_{arom.}$); ^{13}C NMR (DMSO-d_6, 150 MHz): δ/ppm = 145.04 (s), 142.74 (s), 142.69 (d), 141.02 (s), 139.12 (s), 135.43 (d), 133.05 (s), 128.28 (d), 128.14 (d), 126.74 (d), 122.98 (d), 122.82 (s), 118.06 (d), 117.94 (s), 117.71 (d), 104.19 (s); Anal. Calcd for $C_{16}H_8N_3Cl$ (277.5): C, 69.20; H, 2.90; N, 15.13. Found: C, 68.99; H, 2.74; N,15.29.

2.2.2. General method for preparation of compounds 5–7

Compounds **5**–**7** were prepared using microwave irradiation, at optimized power and reaction time, from compound **4** in acetonitrile (10 mL) with a fivefold excess of the corresponding amine. After cooling, the reaction mixture was filtered off to yield pure compounds **5**–**7** as yellow crystals. The details of reaction conditions as well as obtained yield for compound **5** are presented in the Table 2. Compounds **6**–**7** are prepared using similar reaction conditions.

2.2.2.1. 2-Piperidinylbenzimidazo[1,2-a]quinoline-6-carbonitrile

5. Compound **5** was prepared using the above method from **4** (0.050 g, 0.18 mmol) and piperidine (0.09 mL, 0.9 mmol) to yield 0.045 g (85%) of yellow crystals; m.p. 254–256 °C. IR (diamond): ν/cm^{-1} = 2933, 2218, 1608, 1402; ^{1}H NMR (DMSO-d_6, 600 MHz): δ/ppm = 8.56 (s, 1H, $H_{arom.}$), 8.52 (d, 1H, J = 8.22 Hz, $H_{arom.}$), 7.97 (d, 1H, J = 8.23 Hz, $H_{arom.}$), 7.90 (d, 1H, J = 9.09 Hz, $H_{arom.}$), 7.79 (bs, 1H, $H_{arom.}$), 7.63–7.52 (m, 2H, $H_{arom.}$), 7.30 (d, 1H, J = 9.16 Hz, $H_{arom.}$), 3.69–3.62 (m, 6H), 1.67 (t, 4H, J = 6.34 Hz, CH_2); ^{13}C NMR (DMSO-d_6, 150 MHz): δ/ppm = 154.54 (s), 146.27 (s), 144.70 (s), 140.15 (d), 138.82 (s), 132.86 (d), 130.83 (s), 125.27 (d), 123.34 (d), 120.16 (d), 116.90 (s), 115.05 (d), 112.99 (d), 112.31 (s), 97.83 (d), 94.34 (8s), 48.57 (t, 2C), 25.46 (t, 2C), 24.23 (t); Anal. Calcd for $C_{21}H_{18}N_4$ (326.4): C, 77.28; H, 5.56; N, 17.17. Found: C, 77.55; H, 5.78; N,17.09.

2.2.2.2. 2-Pyrrolidinylbenzimidazo[1,2-a]quinoline-6-carbonitrile

6. Compound **6** was prepared using the above method from **4** (0.050 g, 0.18 mmol) and pyrrolidine (0.07 mL, 0.9 mmol) to yield 0.051 g (90%) of yellow crystals; m.p. >295 °C. IR (diamond): ν/cm^{-1} = 2848, 2210, 1608, 1402; ^{1}H NMR (DMSO-d_6, 600 MHz): δ/ppm = 8.54 (s, 1H, $H_{arom.}$), 8.51 (d, 1H, J = 7.92 Hz, $H_{arom.}$), 7.95 (d, 1H, J = 7.71 Hz, $H_{arom.}$), 7.90 (d, 1H, J = 9.03 Hz, $H_{arom.}$), 7.61–7.52 (m, 2H, $H_{arom.}$), 7.44 (s, 1H, $H_{arom.}$), 6.95 (d, 1H, J = 8.88 Hz, $H_{arom.}$), 3.67 (t, 4H, J = 6.68 Hz, CH_2), 2.55 (t, 4H, J = 6.68 Hz, CH_2); ^{13}C NMR (DMSO-d_6, 150 MHz): δ/ppm = 164.63 (s), 153.15 (s), 147.73 (s), 143.82 (s), 142.99 (s), 138.50 (d), 133.60 (d), 130.78 (s), 127.76 (d), 125.27 (d), 124.20 (s), 122.07 (d), 115.15 (d), 113.08 (d), 112.88 (s), 111.76 (d), 48.37 (t, 2C), 25.45 (8t, 2C); Anal. Calcd for $C_{20}H_{16}N_4$ (312.3): C, 76.90; H, 5.16; N, 17.94. Found: C, 77.11; H, 5.33; N,17.82.

Table 1
General and crystal data and summary of intensity data collection and structure refinement for compounds **4** and **5**.

	4	**5**
Formula	$C_{16}H_8ClN_3$	$C_{21}H_{18}N_4$
M_r	277.70	326.39
Crystal system, colour and habit	Monoclinic, yellow, prism	Triclinic, yellow, needle
Space group	$P\,2_1/n$	$P\,\bar{1}$
Crystal dimensions (mm^3)	0.29 × 0.17 × 0.09	0.21 × 0.08 × 0.01
Unit cell parameters:		
a (Å)	9.86860(10)	7.4971(8)
b (Å)	7.23480(10)	10.7027(9)
c (Å)	17.7606(2)	11.0809(15)
α/°		83.13(1)
β/°	102.87(1)	71.14(1)
γ/°		75.95(1)
V (Å^3)	1236.22(3)	815.42(16)
Z	4	2
D_c (g cm^{-3})	1.492	1.329
μ (mm^{-1})	2.654	0.081
F(000)	568	344
θ range for data collection (°)[a]	6–75	3–25
h,k,l range	−11 to 12	−8 to 8
	−9 to 6	−12 to 11
	−20 to 22	−12 to 13
Scan type	ω	ω
No. measured reflections	6134	9973
No. independent reflections ($R_{int.}$)	2479 (0.065)	2825 (0.0356)
No. refined parameters/Restraints	181/0	226/0
No. observed reflections, $I \geq 2\sigma(I)$	2151	1535
g_1, g_2 in w	0.0830, 0.1569	0.1241, 0.5214
R, wR [$I \geq 2\sigma(I)$]	0.0463, 0.1285	0.0838, 0.2861
R, wR [all data]	0.0540, 0.1218	0.1370, 0.2655
Goodness of fit on F^2, S	1.06	1.16
Min. and max. electron density (e Å^{-3})	−0.29, 0.30	−0.29, 0.20
Maximum Δ/σ	0.001	<0.001

[a] The data collection for structures **4** and **5** were carried with Oxford Xcalibur Nova diffractometer with graphite-monocromated λ(CuKα) = 1.54184 Å (compound **4**) and Oxford Xcalibur PX diffractometer with graphite-monocromated λ (MoKα) = 0.71073 Å (compound **5**) at ambient temperature with CCD detectors using ω scan mode.

Table 2
The effect of reaction time on yield of **5** by using a constant power and temperature.

Reaction conditions	Compound **5**						
Time (min)	10	25	60	120	180	240	360
Yield (%)	35	46	54	66	75	80	85

2.2.2.3. 2-Piperazinylbenzimidazo[1,2-a]quinoline-6-carbonitrile 7. Compound **7** was prepared using the above method from **4** (0.050 g, 0.18 mmol) and piperazine (0.78 g, 0.9 mmol) to yield 0.033 g (56%) of yellow crystals; m.p. 192–196 °C. IR (diamond): ν/cm^{-1} = 2920, 2220, 1618, 1454; ^{1}H NMR (DMSO-d_6, 600 MHz): δ/ppm = 8.87 (s, 1H, NH), 8.48 (s, 1H, $H_{arom.}$), 8.43 (d, 1H, J = 8.04 Hz, $H_{arom.}$), 7.94 (d, 1H, J = 8.04 Hz, $H_{arom.}$), 7.83 (d, 1H, J = 8.04 Hz, $H_{arom.}$), 7.66 (s, 1H, $H_{arom.}$), 7.58 (t, 1H, J = 8.20 Hz, $H_{arom.}$), 7.52 (t, 1H, J = 8.22 Hz, $H_{arom.}$), 7.24 (dd, 1H, J_1 = 9.8 Hz, J_2 = 1.45 Hz, $H_{arom.}$), 3.49 (t, 4H, J = 4.52 Hz, CH_2), 2.93 (t, 4H, J = 4.52 Hz, CH_2); ^{13}C NMR (DMSO-d_6, 150 MHz): δ/ppm = 154.12 (s), 145.55 (s), 144.03 (s), 139.66 (d), 137.94 (s), 132.17 (d), 130.18 (s), 124.79 (d), 122.85 (d), 119.61 (d), 116.37 (s), 114.67 (d), 112.22 (d), 112.20 (s), 97.33 (d), 94.24 (s), 47.16 (t, 2C), 44.89 (8t, 2C); Anal. Calcd for $C_{20}H_{19}N_5$ (327.2): C, 73.37; H, 5.23; N, 21.34. Found: C, 73.18; H, 5.15; N, 21.55.

*2.2.3. General method for preparation of compounds **8–10***

A stirred amount of **5–7** (0.15 mmol, 0.11 mmol) in absolute ethanol (10 mL) was cooled in an ice-salt bath and was saturated with HCl gas. The reaction mixture was stirred at the room temperature for 24 h and the obtained product was filtered off and washed with small amount of diethyl-ether (10 mL) to yield powdered products.

2.2.3.1. 2-Piperidinylbenzimidazo[1,2-a]quinoline-6-carbonitrile hydrochloride 8. Compound **8** was prepared using the above method from **5** (0.050 g, 0.15 mmol) to yield 0.045 g (80%) of yellow powder; m.p. 207–211 °C. IR (diamond): ν/cm^{-1} = 3149, 2245, 1598, 1359: ^{1}H NMR (DMSO-d_6, 600 MHz): δ/ppm = 8.96 (s, 1H, $H_{arom.}$), 8.71 (d, 1H, J = 8.07 Hz, $H_{arom.}$), 8.11 (d, 1H, J = 7.77 Hz, $H_{arom.}$), 8.01 (d, 1H, J = 9.18 Hz, $H_{arom.}$), 7.95 (bs, 1H, NH^+), 7.91 (s, 1H, $H_{arom.}$), 7.78–7.67 (m, 2H, $H_{arom.}$), 7.51 (d, 1H, J = 8.82 Hz, $H_{arom.}$), 3.84–3.81 (m, 6H, CH_2), 1.72 (t, 4H, J = 6.30 Hz, CH_2); ^{13}C NMR (DMSO-d_6, 150 MHz): δ/ppm = 165.63 (s), 163.48 (s), 154.26 (s), 143.36 (s), 138.35 (d), 137.28 (s), 133.44 (d, 2C), 128.20 (s), 127.69 (d), 125.42 (d), 117.96 (s), 116.40 (d), 115.44 (d), 114.08 (s), 48.84 (t, 2C), 25.42 (t, 2C), 24.02 (t); Anal. Calcd for $C_{21}H_{19}ClN_4$ (362.9): C, 69.51; H, 5.28; N, 15.44. Found: C, 69.72; H, 5.45; N, 15.21.

2.2.3.2. 2-Pyrrolidinylbenzimidazo[1,2-a]quinoline-6-carbonitrile hydrochloride 9. Compound **9** was prepared using the above method from **6** (0.035 g, 0.11 mmol) to yield 0.034 g (87%) of orange powder; m.p. 264–268 °C. IR (diamond): ν/cm^{-1} = 3149, 2234, 1594, 1332; ^{1}H NMR (DMSO-d_6, 600 MHz): δ/ppm = 8.83 (s, 1H, $H_{arom.}$), 8.57 (d, 1H, J = 7.80 Hz, $H_{arom.}$), 8.06 (d, 1H, J = 7.65 Hz, $H_{arom.}$), 8.04 (bs, 1H, NH^+), 7.95 (d, 1H, J = 8.88 Hz, $H_{arom.}$), 7.70–7.60 (m, 2H, $H_{arom.}$), 7.48 (s, 1H, $H_{arom.}$), 7.03 (d, 1H, J = 7.89 Hz, $H_{arom.}$), 3.60 (t, 4H, J = 6.67 Hz, CH_2), 2.13 (t, 4H, J = 6.69 Hz, CH_2); ^{13}C NMR (DMSO-d_6, 150 MHz): δ/ppm = 165.73 (s), 151.64 (s), 148.72 (s), 144.82 (s), 144.12 (s), 138.24 (d), 137.82 (s), 133.34 (d), 127.50 (d), 126.57 (d), 124.72 (s), 124.20 (d), 116.19 (d), 116.07 (d), 114.13 (d), 112.76 (s), 48.45 (t, 2C), 25.37 (t, 2C); Anal. Calcd for $C_{20}H_{17}ClN_4$ (312.3): C, 68.86; H, 4.19; N, 16.06. Found: C, 69.10; H, 4.36; N, 16.20.

2.2.3.3. 2-Piperazinylbenzimidazo[1,2-a]quinoline-6-carbonitrile hydrochloride 10. Compound **10** was prepared using the above method from **7** (0.050 g, 0.15 mmol) to yield 0.050 g (90%) of yellow powder; m.p. > 280 °C. IR (diamond): ν/cm^{-1} = 3214, 2230, 1604, 1400; ^{1}H NMR (DMSO-d_6, 600 MHz): δ/ppm = 9.65 (brs, 2H, NH, NH^+), 8.59 (s, 1H, $H_{arom.}$), 8.53 (d, 1H, J = 7.74 Hz, $H_{arom.}$), 7.95 (t, 2H, J = 7.14 Hz, $H_{arom.}$), 7.74 (s, 1H, $H_{arom.}$), 7.62 (t, 1H, J = 7.20 Hz, $H_{arom.}$), 7.55 (t, 1H, J = 7.26 Hz, $H_{arom.}$), 7.34 (d, 1H, J = 8.37 Hz, $H_{arom.}$), 4.14 (t, 4H, J = 4.50 Hz, CH_2), 3.32 (t, 4H, J = 4.50 Hz, CH_2); ^{13}C NMR (DMSO-d_6, 150 MHz): δ/ppm = 153.81 (s), 145.48 (s), 142.99 (s), 140.80 (d), 138.10 (s), 132.96 (d), 130.36 (s), 125.64 (d), 123.82 (d), 119.56 (d), 116.43 (s), 115.63 (d), 113.61 (s), 113.46 (d), 98.74 (d), 94.93 (s), 44.35 (t, 2C), 42.78 (t, 2C); Anal. Calcd for $C_{20}H_{18}ClN_5$ (363.1): C, 66.02; H, 4.99; N, 19.25. Found: C, 66.20; H, 5.12; N, 19.45.

2.3. Spectroscopic characterization

UV absorption spectra were recorded, against the solvent, at (25 ± 0.1) °C, using a Varian Cary 50 spectrophotometer operated in double-beam mode. The wavelength range covered was 200–450 nm. Quartz cells of 1-cm path length were used throughout and absorbancies were sampled at 0.1 nm intervals. Fluorescence measurements were carried out on a Varian Cary Eclipse fluorescence spectrophotometer at 25 °C using 1-cm path quartz cells. Excitation maxima were determined from excitation spectra covering the range of 200–450 nm. Emission spectra were recorded from 400 to 600 nm and corrected for the effects of time- and wavelength-dependent light-source fluctuations using a standard of rhodamine 101, a diffuser provided with the fluorimeter and the software supplied with the instrument. The measurements were performed in ethanol (HPLC grade). Relative fluorescence quantum yields were determined according to *Miller* [28] using Eq. (1)

$$\phi_x = \phi_s \times A_s D_x n_x^2 / A_x D_s n_s^2 \quad (1)$$

wherein ϕ is the emission quantum yield, A is the absorbance at the excitation wavelength, D is the area under the corrected emission curve and n is the refractive index of the solvents used. The subscripts s and x refer to the standard and to the unknown, respectively. The standard employed was quinine sulfate with a published fluorescence quantum yield of 0.54 [29]. All samples were purged with argon to displace oxygen. The reproducibility (difference between the largest and the smallest value in a series of three independent measurements, divided by their arithmetic mean) of quantum yield measurements was better than 10%.

2.4. Single-crystal X-ray diffraction experiment

Selected crystallographic and refinement data for structures **4** and **5** obtained by the single-crystal X-ray diffraction experiments are reported in Table 1. Data collection for both structures has been performed by applying the CrysAlis Software system, Version 1.171.33.31 [30]. The Lorentz-polarization effect was corrected and the intensity data reduced by the CrysAlis RED application of the CrysAlis Software system, Version 1.171.33.31 [30]. The diffraction data have been scaled for absorption effects by the multi-scanning method. Structures were solved by direct methods and refined on F^2 by weighted full-matrix least-squares. Programs SHELXS97 and SHELXL97 [30] integrated in the WinGX v. 1.70 [31] software system were used to solve and refine structures. All non-hydrogen atoms were refined anisotropically. Hydrogen atoms belonging to Csp^2 carbon atoms were placed in geometrically idealized positions [Csp^2-H 0.93 Å with $U_{iso}(H) = 1.2\ U_{eq}(C)$] and they were constrained to ride on their parent atoms by using the appropriate SHELXL97 HFIX instructions. The molecular geometry calculations and graphics were obtained using ORTEP-3 [32] integrated in the WinGX software system, PLATON [33] programme and Mercury [34].

2.5. Interaction with ct-DNA

The *calf thymus* DNA (ct-DNA) was purchased from Aldrich, dissolved in sodium cacodylate buffer, I = 0.05 mol dm^{-3}, pH = 7, additionally sonicated and filtered through a 0.45 μm filter and the concentration of corresponding solution determined spectroscopically as the concentration of phosphates. The measurements were performed at room temperature in the aqueous buffer solution

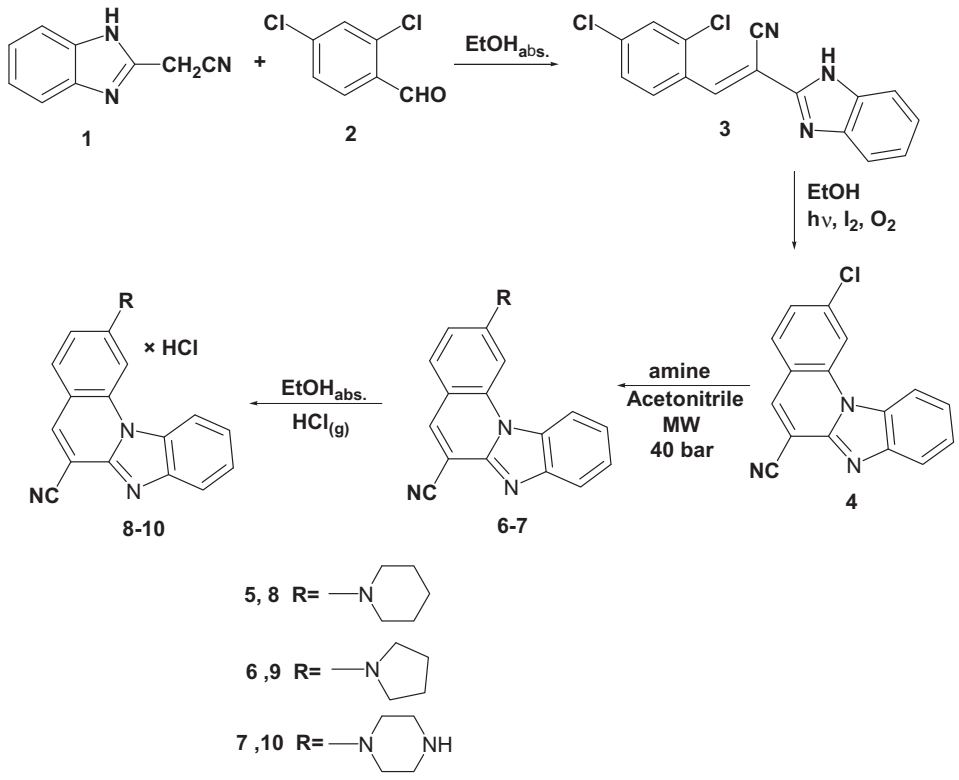

Scheme 1. Synthesis of compounds **3**–**10**.

(pH = 7.0; sodium cacodylate buffer, $I = 0.05$ mol dm^{-3}). Under the experimental conditions used the absorbance and fluorescence intensities of studied compounds were proportional to their concentrations. Obtained data were corrected for dilution. Spectroscopic titrations were performed by adding portions of polynucleotide solution into the solution of the compounds **8**–**10**.

3. Results and discussion

3.1. Synthesis

Compounds **3**–**10** were successfully synthesized according to the Scheme 1. Fused compound **4** was prepared by a previously described method [35], by photochemical dehydrohalogenation of compound **3**.

Benzimidazo[1,2-*a*]quinolines **5**–**7**, substituted with piperidine, pyrrolidine and piperazine nuclei, were prepared by using a microwave irradiation in relative high yields 56–90%. A series of experiments were undertaken in order to optimise the amination reactions of substrate **4** (Table 2). Based on these experiments it was concluded that the optimal yield of **5** (85%, HPLC/MS) was obtained by using 800 W power and 170 °C in MeCN with a fivefold excess of the amine. Compounds **6** and **7** were prepared using identical reaction conditions.

The uncatalyzed amination of compound **4** conducted by conventional heating in EtOH, MeCN or DMF as solvents, after several days, gave compounds **5**–**7** only in very low yields (<10%).

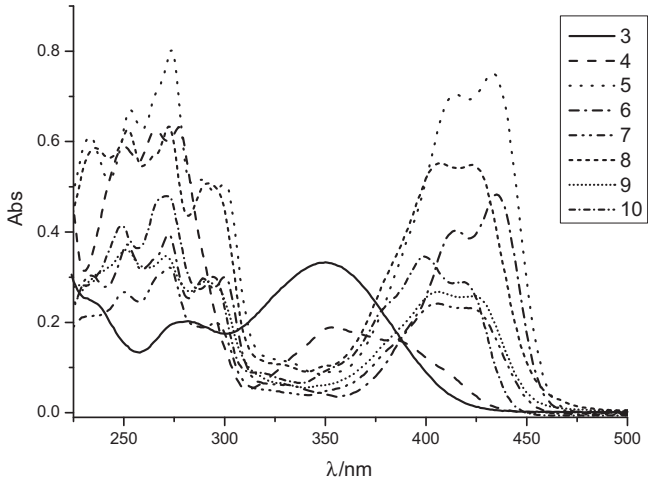

Fig. 1. UV/Vis spectra of compounds **3**–**10**.

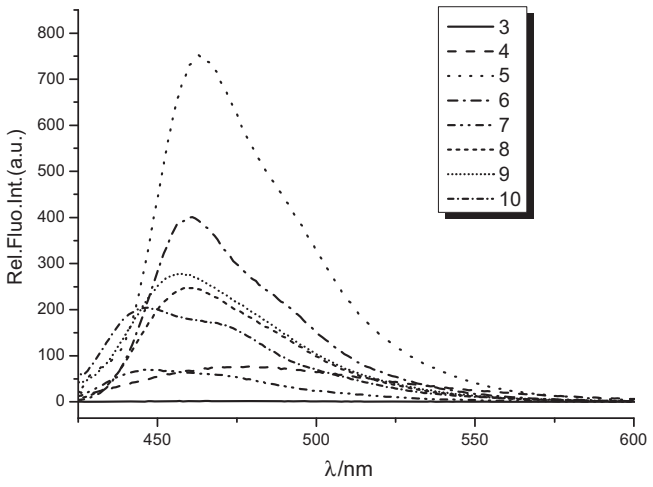

Fig. 2. Fluorescence emission spectra of compounds **3**–**10**.

Table 3
Electronic absorption and fluorescence emission data of compounds **3**–**10** in ethanol.

Comp.	**3**	**4**	**5**	**6**	**7**	**8**	**9**	**10**
λ_{max}/nm		388	432	436	423	422	425	419
	355	350	414	414	404	406	402	399
	283	276	272	300	295	292	290	293
		248	252	289	272	272	270	270
				272	249		250	249
$\varepsilon \times 10^3$ (dm^3 mol^{-1} cm^{-1})		7.5	38.0	24.2	11.7	27.5	12.8	14.5
	20.8	9.0	35.7	19.9	11.9	27.6	13.3	17.1
	7.6	31.2	40.4	14.8	9.8	25.3	14.7	15.0
		28.5	33.8	14.8	16.1	31.7	17.3	24.1
				19.8	13.3			20.5
λ_{emiss}/nm	–	478	464	460	458	459	456	445
								469
Rel. Fluo. Int (arb. un.)	–	78.8	750.1	399.5	13.8	246.4	277.4	202.7
								172.6
ϕ	–	0.545	0.543	0.529	0.756	0.497	0.473	0.607
Stokes shift (nm)	–	202	192	188	186	187	206	175

The results lead us to conclude that the microwave assisted amination provided shorter reaction time, highly increased yield as well as simple product isolation procedure. Hydrochlorides **8**–**10** were prepared to improve the poor solubility of compounds **5**–**7** in water.

The ^{1}H NMR spectrum of the fused benzimidazo[1,2-*a*]quinoline **4** showed no signal for the NH group of benzimidazole nucleus of compound **3**, thus confirming cyclic structure formation. The ^{1}H NMR spectra of amino substituted benzimidazo[1,2-*a*]quinolines **5**–**7** showed a downfield shift of the aromatic protons in comparison to 2-chloro-benzimidazo[1,2-*a*]quinoline-6-carbonitrile **4** and appearance of protons related to piperidine, pyrrolidine or piperazine nuclei. Protonation of compounds **5**–**7** lead to the appearance of signal related to NH^+ group in the ^{1}H NMR spectra of compounds **8**–**10** as well as a downfield shift of protons related to corresponding cyclic amine substituent.

3.2. Spectroscopic characterization

In order to study the spectroscopic properties of prepared compounds **3**–**10**, UV/Vis and fluorescence emission spectra was undertaken in ethanol. The stock solutions of compounds **3**–**10** were prepared in ethanol by concentrations as it follows: *c* (**3**) = 4.46 × 10^{-3} mol dm^{-3}; *c*(**4**) = 1.8 × 10^{-4} mol dm^{-3}; *c* (**5**) = 9 × 10^{-5} mol dm^{-3}; *c*(**6**) = 4 × 10^{-5} mol dm^{-3}; *c* (**7**) = 2.14 × 10^{-3} mol dm^{-3}; *c*(**8**) = 1.52 × 10^{-3} mol dm^{-3}; *c* (**9**) = 3.8 × 10^{-4} mol dm^{-3}; *c*(**10**) = 2.0 × 10^{-4} mol dm^{-3}; UV/Vis spectra of prepared compounds were recorded at the same concentration of 2.0 × 10^{-5} mol dm^{-3} and can be visualized in Fig. 1. Precursor **3** showed one intense main absorption band at 355 nm while compound **4** showed several absorption bands, especially intense in the region from 250 to 280 nm with high extinction coefficients. Most of these electronic transitions are made from π to π* orbitals of tetracyclic conjugated π-system.

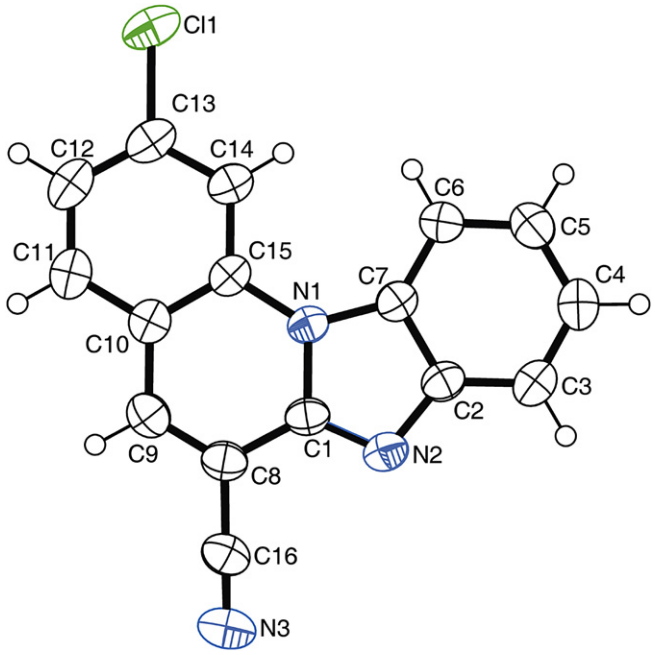

Fig. 3. ORTEP drawing of molecular structure of 4 with atom labeling scheme. The displacement ellipsoids are drawn at the 50% probability level at 296 K.

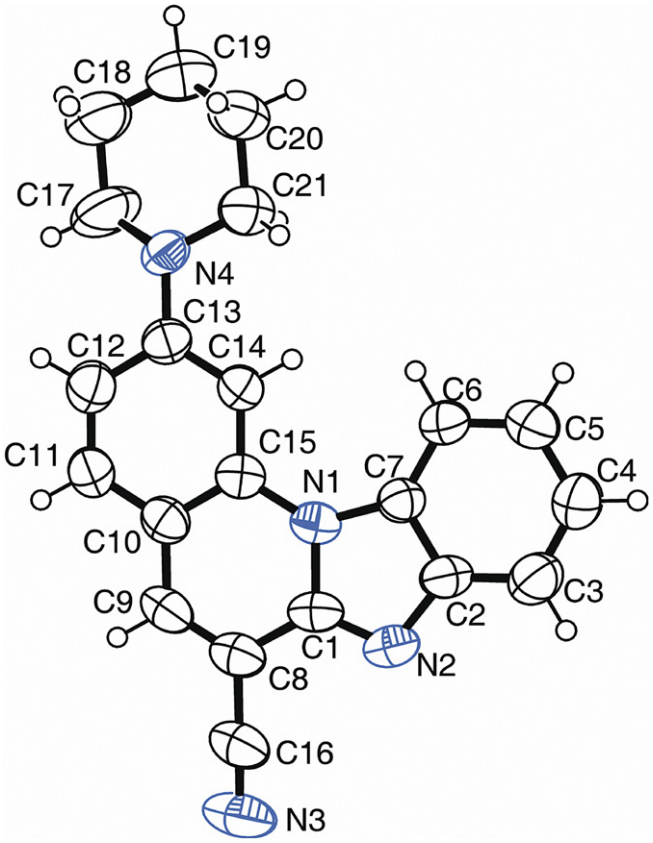

Fig. 4. ORTEP drawing of molecular structure of 5 with atom labeling scheme. The displacement ellipsoids are drawn at the 50% probability level at 296 K.

Conversion of chlorine into the piperidine, pyrrolidine or piperazine substituents resulted in strong bathochromic shift of ~50 nm and an increasing in the molar extinction coefficient. Heteroatoms with non-bonding electrons, such as nitrogen, can absorb UV radiation when the electrons make a transition from *n* orbitals to π* orbitals. The non-bonding electrons of nitrogen can take part in the resonance of the tetracyclic aromatic structure which causes a bathochromic shift in the absorbance maximum.

Compared with **6**–**7** and **9**–**10**, with the pyrrolidine and piperazine substituents, **5** and **8** with the piperidine substituent showed a hyperchromic effect. This may be explained by the fact that N-atom in cyclic amines approximates a planar arrangement during the facile interconversion between ring forms, especially in more polar solvents. The interconversion is more rapid for piperidine derivatives than other cyclic amines, a feature which is also suggested in some previous studies [36].

Fluorescence emission spectra were recorded at the same concentration of 5.0×10^{-8} mol dm^{-3} and can be visualized in Fig. 2. Fluorescence excitation was performed at the wavelength of maximum absorption. Compounds **4**–**9** exhibit characteristic fluorescence emission with maxima at about 470 nm and show single emission band while compound **10** showed two emission bands. Compound **3** did not show any emission band under the applied conditions. Hydrochloride salts **8**–**10** showed a hypsochromic shift and lower fluorescence intensity than compounds **5**–**7**.

Electronic absorption and fluorescence data of compounds **3**–**10** recorded at the same concentration in ethanol, quantum yield data φ and Stokes shift values are summarised in Table 3. Excitation spectra of all studied compounds are in a good agreement with their absorption spectra. The difference in energy between the absorbed and emitted radiation is known as the Stokes shift. All benzimidazo[1,2-*a*]quinolines **4**–**10** presented large Stokes shift values (175–206 nm) which could be generally attributed to a different charge distribution (or geometry) in the excited state of molecules compared to the ground state.

3.3. Crystal structure study of compounds *4* and *5*

ORTEP images (50% of atomic displacement parameters) of compounds **4** and **5** are depicted in Fig. 3 (compound **4**) and Fig. 4 (compound **5**), while crystal packing structures are shown in Figs. 5 and 6 for compounds **4** and **5**, respectively. The selected molecular geometry is listed in Table 4 and hydrogen bonding geometry and π···π interactions in Tables 5 and 6, respectively. The molecules of **4** and **5** are essentially planar (except piperidine substituent at C13 atom in **5**). The dihedral angles calculated between the two planes defined by atoms N1 N2 C1 C2 C3 C4 C5 C6 and C7 (one plane) and N1 C1 C8 C9 C10 C11 C12 C13 C14 and C15 (another plane) amount 2.0(1)° and 2.9(2)° for **4** and **5**, respectively. These values are comparable for similar benzimidazo[1,2-*a*]quinoline molecular systems substituted at position 2 with the angle range 0.65(6)o [29]–4.27(4)° [7]. The piperidine substituent at C13 in **5** is rotated around C13-N4 single bond (Table 4) by 14.0(3)° implicating that the molecule as a whole is not planar. The benzimidazo[1,2-*a*]

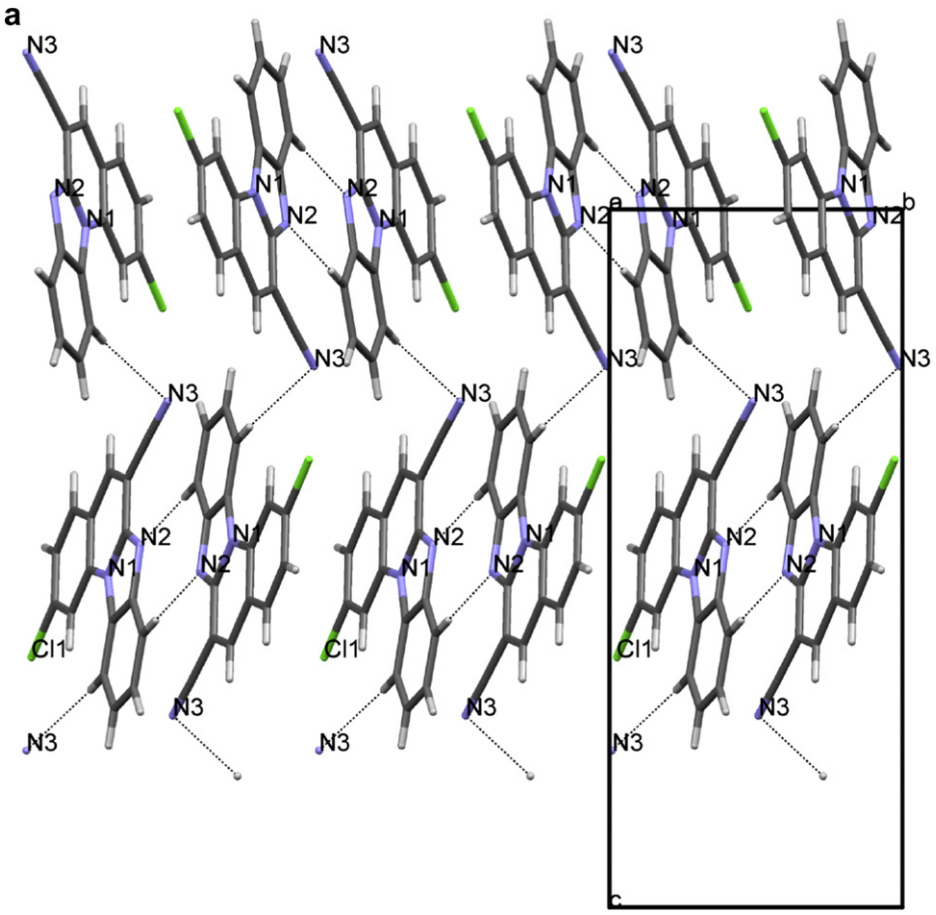

Fig. 5. a) Mercury drawing of crystal structure of 4 viewed down *a* axis. The intermolecular hydrogen bonds of the C–H···N type are shown by dashed lines. Imidazole N2 nitrogen atom participates into C–H···N hydrogen bond which links molecules into discrete dimers spreading along *b* axis, while cyano N3 nitrogen atoms forms another C–H···N hydrogen bond which further joins dimers along *c* axis. In such way, the layers are formed.

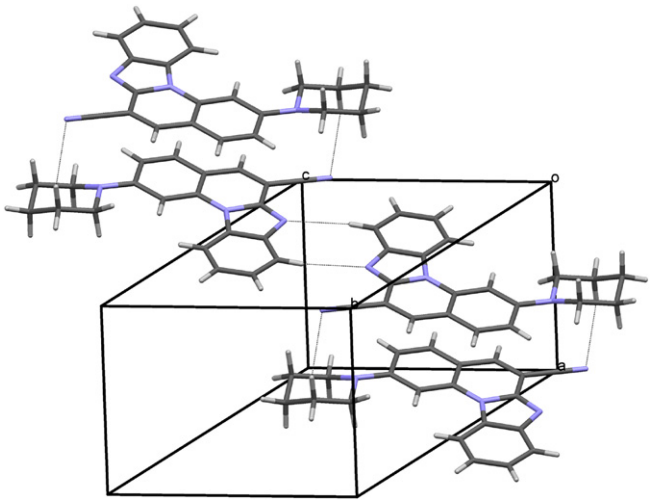

Fig. 6. Mercury drawing of crystal structure of 5. The intermolecular hydrogen bonds of the C–H···N type are shown by dashed lines. The molecules are mutually connected by two different types of rings which alternate thus forming the chains of rings.

quinoline fragment in **4** and **5** contains sp^3 hybridized N1 atom which lone pair electrons are delocalized within the π-system of fused rings. The C–N bond distances with the sp^3 hybridized N1 atom (C15–N21, C1–N1 and C7–N1) are significantly longer then C–N bonds formed by the sp^2 hybridized N2 atom (shorter C1–N2 and longer C2–N2 in imidazolyl ring), which are dominantly π in character (Table 4), as it is found in analogous benzimidazo[1,2-*a*] quinolines [7,37].

The intermolecular contacts are characterized by weak C–H···N hydrogen bonds formed between phenyl –CH groups and imidazole sp^2 hybridized N2 atom or the N3 atom of the cyano group (Table 5). The C3–H3···N2 intermolecular hydrogen bond is found in both structures **4** and **5**, while in **4** the proton acceptor cyano N3 atom participates in hydrogen bond formation with phenyl –CH group, and in **5** with less acidic methylene $-CH_2$ group of piperidine ring. The analogous hydrogen bonding arrangement has been observed in the crystal structures of benzimidazo[1,2-*a*] quinolines [7,37]. The π···π aromatic stacking [38–41] in **4** and **5** are not analogous. The π···π aromatic stacking interactions are found between the imidazole and phenyl ring of quinoline fragment as well as between imidazole and N1, C1, C8, C9, C10 and C15 atoms of quinoline ring in **4**, while in **5** the condensed benzimidazolyl heterocyclic rings are included (see Table 6 for ring atoms).

Table 4
Selected interatomic distances (Å) and valence and torsion angles (°) for the compounds **4** and **5**.

	Selected bond distances	
	4	**5**
Cl1–C13 (C13–N4 in **5**)	1.7334(17)	1.398(5)
C1–N2	1.305(2)	1.307(6)
C2–N2	1.384(2)	1.394(6)
C1–N1	1.403(2)	1.398(5)
C15–N1	1.407(2)	1.400(6)
C7–N1	1.396(2)	1.400(5)
C16–N3	1.144(2)	1.127(6)
	Bond angles	
C8–C1–N2	127.4(1)	127.1(4)
C1–N2–C2	104.8(1)	104.4(4)
C15–N1–C7	132.8(1)	133.2(3)
C8–C16–N3	178.2(2)	178.7(7)

Table 5
Hydrogen bond geometry (Å, °) for compounds **4** and **5**.

D–H···A	D–H	H···A	D···A	∠D–H···A	Symmetry code
4					
C6–H6···N3	0.93	2.540	3.376(3)	150	$1/2 + x,1/2 - y,1/2 + z$
C3–H3···N2	0.93	2.649	3.571(2)	171	$x + 1/2,-y + 1/2,+z + 1/2$
5					
C20–H20A···N3	0.97	2.670	3.591(9)	159	$-x + 1,-y + 1,-z$
C3–H3···N2	0.93	2.645	3.561(8)	168	$-x + 1,-y + 1,-z$

3.4. Interaction with ct-DNA

Interaction of compounds **8**–**10** as hydrochloride salts with ct-DNA was studied using fluorescence spectroscopy. Compounds **8**–**10** could interact with ct-DNA resulting in an increase in fluorescence intensity. In such a way **8**–**10** could be used for a possible application as fluorescent probes for DNA detection. Stock solutions of compounds **8** and **9** were prepared in DMSO, c (**8**) = 1.65 mol dm^{-3}; c(**9**) = 4.8 × 10^{-4} mol dm^{-3} while stock solution of compound **10** was prepared in H_2O, c (**10**) = 1.38 × 10^{-4} mol dm^{-3}. Stock solutions of compounds **8**–**10** were stable over longer periods (60 days).

Small aliquots of DMSO stock solutions were added into the aqueous medium for compounds **8** and **9** providing that DMSO content in experiments was less than 1%.

The interaction with ct-DNA was performed in aqueous buffer at pH 7 at compound concentrations of 5.0 × 10^{-7} mol dm^{-3} [7,42,43]. The effects on emission maxima of **8**–**10** upon the addition of ct-DNA are presented in Fig. 7.

Interactions of compound **8**–**10** with ct-DNA were measured at different ratios r ((compound)/(ct-DNA)) followed by increasing concentration of added ct-DNA up to high excess of ct-DNA. The changes of fluorescence intensity on emission maxima for compounds **8**–**10** upon the addition of corresponding amounts of ct-DNA are presented in Table 7.

Table 6
Geometrical parameters of π···π interactions[a] (Å, °) for compounds **4** and **5**.

Interaction[b]	C_g–C_g distance	C_g···P1[b]	C_g···P2[c]	α[d]	β[e]	Slippage
4						
Cg3···Cg4^{i}	3.634(1)	−3.351(1)	−3.338(1)	1.09(8)	23.30	1.437
Cg3···Cg6^{i}	3.601(1)	−3.353(1)	−3.375(1)	1.07(8)	20.42	1.256
Cg3···Cg6^{ii}	3.725(1)	3.394(1)	3.403(1)	1.07(8)	24.00	1.515
Cg4···Cg4^{i}	3.564(1)	−3.351(1)	−3.351(1)	0	19.91	1.214
Cg4···Cg6^{ii}	3.651(1)	3.383(1)	3.386(1)	0.32(7)	21.96	1.365
5						
Cg6···Cg7^{iii}	3.746(3)	−3.513(2)	−3.527(2)	3.2(2)	19.71	1.263
Cg7···Cg7^{iv}	4.029(3)	3.522(2)	3.521(2)	0	29.07	1.958

[a] Those possible interactions for which perpendicular distance between two planes is longer than 3.8 Å (3.3–3.8 Å) (C_g···P1 and C_g···P2; the perpendicular distance of corresponding centroid to a plane) and dihedral angles (between P1 and P2) larger than 20° are not taken into account. The calculated slippage on the basis of Cg···Cg distances as well as the value of the angle between Cg···Cg vector and vertical line on corresponding plane has been taken into account as one of the geometrical criteria, too (approx. 1.5 Å for π···π stacking interactions).

[b] Rings Cg3, Cg4 and Cg6 are defined by the atoms N1, C1, N2, C2 and C7; N1, C1, C8, C9 C10 and C15; C10, C11, C12, C14, C14 and C15 in **4**, respectively. Rings Cg6 and Cg7 are defined by the atoms N1, C1, N2, C2, C3, C4, C5, C6 and C7; N1, C7, C2, N2, C1, C8, C9, C10 and C15 in **5**, respectively.

[c] C_g···P1 (or P2) is the perpendicular distance of corresponding centroid to a plane. Planes P1 or P2 are defined by the atoms, which define the corresponding centroids.

[d] Dihedral angles between P1 and P2.

[e] β is the angle between Cg···Cg vector and vertical line on corresponding plane. Symmetry codes: $i = 2 - x,-y,-z$, ii = $2 - x,1 - y,-z$, iii = $x,1 - y,-z$; iv = $1 - x,1 - y,-z$.

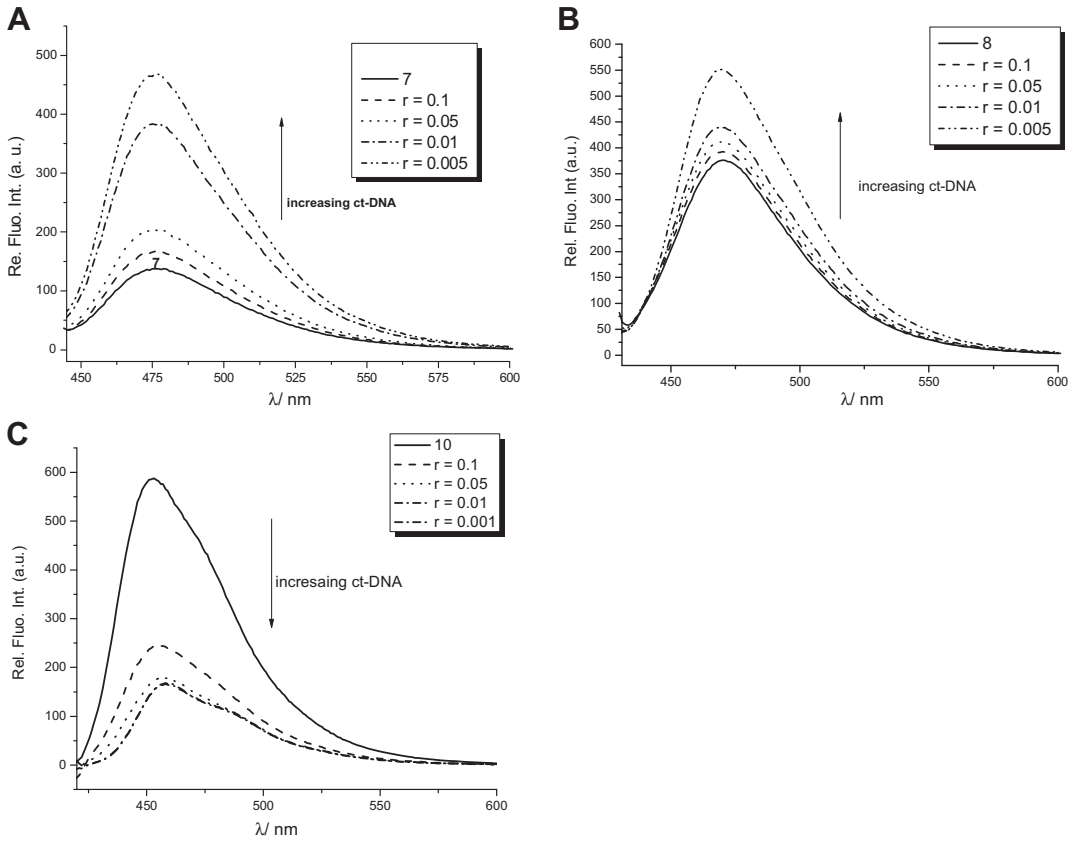

Fig. 7. Fluorescence emission spectra of compounds **8** (A), **9** (B) and **10** (C) in the presence of different ratios r of ct-DNA at compounds concentration of $c = 5 \times 10^{-7}$ mol dm^{-3} excited on the wavelength of absorption maxima.

In aqueous buffered solution, significant changes in the emission spectra of compounds **8**–**9** occurred during the addition of small aliquots of ct-DNA. These changes resulted in a strong hyperchromic shift with fluorescence enhancement and without any changes in the wavelength of emission maxima. The addition of ct-DNA to compounds **8** and **9** with piperidine and pyrrolidine substituents increased the fluorescence intensity by ca. 3.38 and 1.47 times, respectively. Thus, both compound **8** and **9** offer possible applications for DNA detection in biological systems as fluorescence probes since they exhibit high binding affinity to DNA resulted in fluorescence enhancement as well as intense fluorescence. As it can be viewed in fluorescence emission spectra which represents interaction of compound **10** with ct-DNA (Fig. 7C), compound **10** showed strong hypochromic shift by increasing concentration of ct-DNA as well as a slight bathochromic shift of 5 nm. Above mentioned results are in good agreement with the previously published ones. Namely, our previously published results have shown that positively charged benzimidazo[1,2-*a*]quinolines intercalate into ds DNA since this chromophore posses a planar, highly conjugated tetracyclic aromatic structure which has the ability to intercalate into double helix of DNA molecule. Additional positively charged groups attached to this chromophore, like cyclic amine substituents in compounds **8**–**10**, would be expected to form additional binding interactions.

Based on obtained experimental results, together with previously published ones, we can suggest that the possible mechanism of interaction between the fluorescent probes **8**–**10** and ct-DNA could be intercalation.

Table 7
Fluorescence intensity changes of compounds **8**–**10** upon the addition of ct-DNA at different ratio r ((compound)/(ct-DNA)) at pH = 7.0 (Buffer Na-Cacodylate, $I = 0.05$ mol dm^{-3}).

	r[a]	Re. Fluo. Int/(a.u.)	ΔInt/(a.u.)	F/F_0[b]
8	0	138.2	–	–
	0.1	167.6	29.4	1.21
	0.05	202.3	64.1	1.46
	0.01	384.8	246.6	2.78
	0.005	467.0	328.8	3.38
9	0	375.7	–	–
	0.1	392.2	16.5	1.04
	0.05	409.2	33.5	1.09
	0.01	441.3	65.6	1.17
	0.005	552.6	176.9	1.47
10	0	588.2	–	–
	0.1	245.1	343.1	2.40
	0.05	179.0	409.2	3.29
	0.01	165.2	423.0	3.56
	0.005	165.0	423.2	3.56

[a] r=(compound)/(ct-DNA).
[b] F = fluorescence of compound-DNA complex; F_0 = fluorescence of compound without ct-DNA addition.

4. Conclusions

The main aim of this study was to prepare amino substituted benzimidazo[1,2-*a*]quinolines **5**–**7** in good yields. Their hydrochloride salts **8**–**10** were prepared by protonation with HCl gas to enhance their solubility for spectroscopic characterization of their interaction with ct-DNA. The benzimidazo[1,2-*a*]quinolines **4**–**10** showed interesting spectroscopic properties with several absorption bands. In comparison with compound **4**, aminated compounds

5–**7** and hydrochloride salts **8**–**10** showed strong bathochromic shift of λ_{max} in the absorption spectrum. Fluorescence emission spectra revealed the fact that all compounds, except compound **3**, showed a single emission band with maxima at ca. 470 nm.

The crystal structures of two compounds **4** and **5** have been determined in order to confirm molecular planarity in the crystalline state (it is within 3°, except the piperidine ring in **5** which is rotated around C–N single bond up to 14°) and to reveal possible types of hydrogen bonding interactions. The molecular assembly is dominated by the weak C–H···N intermolecular hydrogen bonds as well as π···π aromatic stacking.

To estimate the probability for possible application of compounds **8**–**10** for DNA detection as fluorescent probes, their interaction with ct-DNA was investigated. Addition of different ratios *r* of ct-DNA to the aqueous buffered solutions of **8** and **9** induced the increase of fluorescence intensity, while compound **10** induced a decrease in fluorescence intensity. The piperidine-substituted compound **8** exhibited the longest fluorescence enhancement. The results revealed a possible application of the compounds **8** and **9** as fluorescent probes for DNA detection.

Acknowledgments

This study was supported by grants 125-0982464-1356 and 098-1191344-2943 by the Ministry of Science, Education and Sports of the Republic of Croatia. G.P. wishes to thank to Dubravka Šišak, PhD student at ETH Laboratory for Crystallography, Wolfgang Pauli str. 10, 8039 Zürich, Switzerland for kindly providing X-ray data collection of compound **5** on Oxford Xcalibur PX diffractometer.

Appendix. Supplementary material

CCDC numbers 774469 & 774470 for compounds **4** and **5** respectively, contains the supplementary crystallographic data for this paper. These data can be obtained free of charge at www.ccdc.cam.ac.uk/conts/retrieving.html [or from the Cambridge Crystallographic Data Centre (CCDC), 12 Union Road, Cambridge CB2 1EZ, UK; fax: +44(0)1223 336033; email: deposit@ccdc.cam.ac.uk]. Structure factors table is available from the authors.

References

[1] Silverman RB. The organic chemistry of drug design and drug action. 2nd ed. Elsevier/Academic Press; 2004.
[2] Demeunynck M, Bailly C, Wilson WD. DNA and RNA binders. Weinheim: Wiley-VCH; 2002.
[3] Demirayak S, Abu Mohsen U, Cagri Karaburun A. Synthesis and anticancer and anti-HIV testing of some pyrazino[1,2-*a*]benzimidazole derivatives. European Journal of Medicinal Chemistry 2002;37:255–60.
[4] Hranjec M, Starčević K, Piantanida I, Kralj M, Marjanović M, Hasani M, et al. Synthesis, antitumor evaluation and DNA binding studies of novel amidino-benzimidazolyl substituted derivatives of furyl-phenyl and thienyl-phenyl-acrylates, naphthofurans and naphthothiophenes. European Journal of Medicinal Chemistry 2008;43:2877–90.
[5] Starčević K, Kralj M, Ester K, Sabol I, Grce M, Pavelić K, et al. Synthesis, antiviral and antitumor activity of 2-substituted-5-amidino-benzimidazoles. Bioorganic & Medicinal Chemistry 2007;15:4419–26.
[6] Brana MF, Castellano JM, Keilhauer G, Machuca A, Martín Y, Redondo C, et al. Anti-Cancer Drug Design 1994;9:527–38.
[7] Hranjec M, Pavlović G, Marjanović M, Kralj M, Karminski-Zamola G. Benzimidazole derivatives related to 2,3-acrylonitriles, benzimidazo[1,2-*a*]quinolines and fluorenes: synthesis, antitumor evaluation *in vitro* and crystal structure determination. European Journal of Medicinal Chemistry; 2010.
[8] Deady LW, Rodemann T, Finlay GJ, Baguley BC, Denny WA. Synthesis and cytotoxic activity of carboxamide derivatives of benzimidazo[2,1-*a*]isoquinoline and pyrido[3',2':4,5]imidazo[2,1-*a*]isoquinoline. Anti-Cancer Drug Design 2000;15:339–46.
[9] Hranjec M, Kralj M, Piantanida I, Sedić M, Šuman L, Pavelić K, et al. Novel cyano- and amidino-substituted derivatives of styryl-2-benzimidazoles and benzimidazo[1,2-a]quinolines. Synthesis, photochemical synthesis, DNA binding and antitumor evaluation, part 3. Journal of Medicinal Chemistry 2007;50:5696–711.
[10] (a) Saçzewski F, Stencel A, Bieńczak AM, Langowska KA, Michaelis M, Werel W, et al. Structure-activity relationships of novel heteroaryl-acrylonitriles as cytotoxic and antibacterial agents. European Journal of Medicinal Chemistry 2008;43:1847–57;
(b) Nandhikonda P, Heagy MD. Dual fluorescent N-aryl-2,3-naphthalimides: applications in ratiometric DNA detection and white organic light-emitting devices. Organic Letters; 2010:4796–9.
[11] Langer R. Perspectives: drug delivery-drugs on target. Science 2001;293:58–9.
[12] Vivas-Mejía P, Rodríguez-Cabán JL, Díaz-Velázquez M, Hernández-Pérez MG, Cox O, Gonzalez FA. DNA binding-independent anti-proliferative action of benzazolo[3,2-α]quinolinium DNA intercalators. Molecular and Cellular Biochemistry 1997;177:69–77.
[13] Chaires JB. Drug-DNA interactions. Current Opinion in Structural Biology 1998;8:314–20.
[14] Hirano K, Oderaotoshi Y, Minataka S, Komatsu M. Unique fluorescent properties of 1-aryl-3,4-diphenylpyrido[1,2-a]benzimidazoles. Chemistry Letters; 2001:1262–3.
[15] Kumar C, Turner R, Ascuncion E. Groove binding of a styrylcyanine dye to the DNA double helix: the salt effect. Journal of Photochemistry and Photobiology A: Chemistry 1993;74:231–8.
[16] Kovalska VB, Kryvorotenko DV, Balanda AO, Losytskyy MY, Tokar VP, Yarmoluk SM. Fluorescent homodimer styrylcyanines: synthesis and spectraleluminescent studies in nucleic acids and protein complex. Dyes and Pigments 2005;67:47–54.
[17] Caddick S, Fitzmaurice R. Microwave enhanced synthesis. Tetrahedron 2008;65:3325–55.
[18] Shi L, Wang M, Fan CA, Zhang FM, Tu YQ. Rapid and efficient microwave-assisted amination of electron-rich aryl halides without a transition-metal catalyst. Organic Letters 2003;19:3515–7.
[19] Salmoria GV, Dall'Oglio E, Zucco C. Aromatic nucleophilic substitutions under microwave irradiation. Tetrahedron Letters 1998;39:2471–4.
[20] Qu G, Han S, Zhang Z, Geng M, Xue F. Microwave assisted synthesis of 6-substituted aminopurine analogs in water. Journal of Brazilian Chemical Society 2006;17:915–22.
[21] Kappe CO, Dallinger D, Murphree SS. Practical microwave synthesis for organic chemists. Weilheim: Wiley-VCH; 2009.
[22] Van der Eycken E, Kappe CO. Microwave-assisted synthesis of heterocycles. Topics in heterocyclic chemistry. Berlin: Springer; 2006.
[23] Shenoy VU, Sesardi S. Synthesis of benzimidazo-[1,2-*a*]-quinolines: fluorescent disperse dyes. Dyes and Pigments 1989;11:137–45.
[24] Brańa MF, Castellano JM, Keilhaurer G, Machuca A, Martin Y, Redondo C, et al. Benzimidazo[1,2-*c*]quinazolines: a new class of antitumor compounds. Anti-Cancer Drug Design 1994;9:527–38.
[25] Pereira MF, Thiéry V, Besson T. Microwave-assisted regioselective N-alkylation of cyclic amidines. Tetrahedron Letters 2007;48:7657–9.
[26] Arienzo R, Cramp S, Dyke HJ, Lockey PM, Norman D, Roach AG, et al. Quinazoline and benzimidazole MCH-1R antagonists. Bioorganic & Medicinal Chemistry Letters 2007;17:1403–7.
[27] Cai Q, Li Z, Wei J, Fu L, Ha C, Pei D, et al. Synthesis of aza-fused polycyclic quinolines through copper-catalyzed cascade reactions. Organic Letters 2010;12:1500–3.
[28] Miller JN. Standards for fluorescence spectrometry. London: Chapman and Hall; 1981.
[29] Eaton DF. Reference materials for fluorescence measurement. Pure & Applied Chemistry 1988;60:1107–14.
[30] Oxford Diffraction Ltd. Xcalibur CCD system, CrysAlis software system, versions 1.171.32.24 and 1.171.33.41. Oxfordshire, England: Abingdon; 2008.
[31] Sheldrick GM. A short history of SHELX. Acta Crystallographica 2008;A64:112–22.
[32] Farrugia LJ. Ortep-3 for Windows (v. 1.08) – a version of the current release of ORTEP-III, which incorporates a Graphical User Interface (GUI). Journal of Applied Crystallography 1997;30:565.
[33] Spek LA. Multipurpose crystallographic tool. Journal of Applied Crystallography 2003;36:7–13.
[34] Macrae CF, Bruno IJ, Chisholm JA, Edgington PR, McCabe P, Pidcock E, et al. Mercury CSD 2.0-new features for the visualization and investigation of crystal structures. Journal of Applied Crystallography 2008;41:466–70.
[35] Hranjec M, Karminski-Zamola G. Synthesis of novel benzimidazolyl substituted acrylonitriles and amidino substituted benzimidazo[1,2-a]quinolines. Molecules 2007;12:1817–28.
[36] (a) Saha S, Samanta A. Influence of the structure of the amino group and polarity of the medium on the photophysical behavior of 4-amino-1,8-naphthalimide derivatives. Journal of Physical Chemistry A 2002;106:4763–71;
(b) Wu L, Burgess K. Synthesis and spectroscopic properties of rosamines with cyclic amine substituents. Journal of Organic Chemistry 2008;73:8711–8.
[37] Hranjec M, Pavlović G, Karminski-Zamola G. Crystal structure and synthesis of benzimidazole substituted acrylonitriles and benzimidazo[1,2-*a*]quinolines. Structural Chemistry 2009;20:91–9.
[38] Hunter CA, Sanders JKM. The nature of π–π interactions. Journal of American Chemical Society 1990;112:5525–34.
[39] Curtis MD, Cao J, Kampf JW. Solid-state packing of conjugated oligomers: from π-stacks to the herringbone structure. Journal of American Chemical Society 2004;126:4318–28.

[40] Hunter CA. The role of aromatic interactions in molecular recognition. Chemical Society Reviews 1994;23:101–9.
[41] Hunter CA, Lawson KR, Perkins J, Urch CJ. Aromatic interactions. Journal of Chemical Society, Perkin Transactions 2001;2:651–69.
[42] Hranjec M, Piantanida I, Kralj M, Šuman L, Pavelić K, Karminski-Zamola G. Novel amidino-substituted thienyl- and furyl-vinyl-benzimidazole derivatives and their photochemical conversion into corresponding diaza-cyclopenta[c]fluorenes. Synthesis, interactions with DNA and RNA and antitumor evaluation. Part 4. Journal of Medicinal Chemistry 2008;51:4899–910.
[43] Starčević K, Hranjec M, Carić D, Karminski-Zamola G. Synthesis and spectroscopic properties of new furyl-phenyl-acrylates and naphthofurans and their interaction with ct-DNA. Monatshefte für Chemie-Chemical Monthly 2008;139:975–83.